

Supporting Information

Stepwise Chelation-Etching Synthesis of Carbon-Confined Ultrafine SnO₂ Nanoparticles for Stable Sodium Storage

Yuanjie Zhang,^a Jiashen Meng,^a Xuanpeng Wang,^a Xiong Liu,^a Xiaoming Xu,^a Ziang Liu,^a Kwadwo Asare Owusu,^a Congyun Huang,^b Qi Li^{*a} and Liqiang Mai^{*a}

^aState Key Laboratory of Advanced Technology for Materials Synthesis and Processing, Wuhan University of Technology, Wuhan 430070, Hubei, China.

^bSchool of Materials Science and Engineering, Wuhan University of Technology, Wuhan 430070, Hubei, China.

Experimental

Preparation of CoSn(OH)₆ nanocubes

1.40 g tin chloride pentahydrate (SnCl₄·5H₂O) was dissolved in 20 mL H₂O to obtain a homogeneous light red solution (named as solution A). 0.9517 g cobalt chloride hexahydrate (CoCl₂·6H₂O) and 1.1864 g sodium citrate dihydrate (Na₃C₆H₅O₇·2H₂O) were dissolved in 120 mL H₂O to obtain a homogeneous solution (named as solution B). 1.60 g sodium hydroxide (NaOH) was dissolved in 20 mL H₂O to obtain a homogeneous solution (named as solution C). Solution A was added into solution B, forming a light pink turbid liquid; then solution C was added dropwise followed by stirring for 1 h. Finally, pink CoSn(OH)₆ powder was obtained after washing and drying in oven at 70 °C for 12 h.

Preparation of CoSn(OH)₆@polydopamine nanocubes

336 mg CoSn(OH)₆ powder and 406.5 mg tris(hydroxymethyl)aminomethane was dissolved in 330 mL H₂O to obtain a light pink turbid liquid, then diluted hydrochloric acid was added to the light pink CoSn(OH)₆ turbid liquid dropwise until the pH value reached 8.5. 100.8 mg dopamine hydrochloride powder was dissolved in 6 mL H₂O, forming colorless solution; then it was added to the light pink CoSn(OH)₆ turbid liquid followed by stirring for 24 h. Finally, the greyish-black CoSn(OH)₆@polydopamine powder was obtained after washing and drying in oven at 70 °C for 12 h.

Preparation of CoSnO₃@NC nanocubes

The as-prepared CoSn(OH)₆@polydopamine powder was annealed at 500 °C (3 °C min⁻¹) under the nitrogen atmosphere for 1 h. Then, the black CoSnO₃@NC powder was obtained.

Preparation of SnO₂@NC nanocubes

75 mg CoSnO₃@NC composite (0.3mmol, based on the molar of Co) and a certain amount of ethylenediaminetetraacetic acid (EDTA) were added to 70 mL H₂O and stirred under sonication for 10 min. Then the black turbid liquid was transferred into 100 mL Teflon-lined sealed autoclave and maintained at 120 °C for 12 h. Afterward, the autoclave was cooled down to room temperature naturally and the samples were washed with distilled water 6 times. The final products were dried at 70 °C for 12 h in an oven. SnO₂@NC-1, SnO₂@NC-1.2, SnO₂@NC-1.5, SnO₂@NC-2 respectively correspond to the product obtained when the additive amount of EDTA is 87.67 mg (0.3 mmol, M_{CoSnO₃}:M_{EDTA}=1:1), 105.2 mg (0.36 mmol, M_{CoSnO₃}:M_{EDTA}=1:1.2), 131.5 mg (0.45 mmol, M_{CoSnO₃}:M_{EDTA}=1:1.5), 175.34 mg (0.6 mmol, M_{CoSnO₃}:M_{EDTA}=1:2).

Characterization

The crystallographic information of the final products were measured using a Bruker D8 Discover X-ray diffractometer (XRD) equipped with a Cu-K α radiation source; the samples were scanned over a 2 θ range from 20° to 80° at room temperature. Scanning electron microscope (SEM) images were collected using a JEOL-7100F SEM. Transmission electron microscope (TEM) and high-resolution TEM (HRTEM) images were collected using a JEM-2100F TEM. The Brunauer-Emmett-Teller (BET) specific surface area was calculated from nitrogen adsorption isotherms measured at 77 K using a Tristar-3020 instrument. Energy-dispersive X-ray spectra (EDS) was recorded using an Oxford IE250 system. X-ray photoelectron spectroscopy (XPS) measurements were performed using a VG MultiLab 2000 instrument. Thermogravimetric analysis (TGA) was performed using a Netzsch STA 449 C simultaneous analyzer under an air flow with a temperature ramp of 10 °C min⁻¹. Raman spectra was obtained using a Renishaw INVIA micro-Raman spectroscopy system. Fourier transform infrared spectroscopy (FTIR) was recorded using a Thermo

Nicolet Nexus instrument. Inductively coupled plasma atomic emission spectrometry (ICP-AES) was performed using an Optima 4300DV instrument.

Electrochemical measurements

Typical 2016 coin cells were assembled in an argon-filled glovebox with moisture and oxygen concentrations below 1.0 ppm. Sodium foil was used as the counter electrode and a solution of NaClO_4 (1 M) in EC: DMC = 1:1 (Vol %) with 5 wt.% FEC was used as the electrolyte. The anode was composed of a grinded mixture of 70 wt.% active material, 20 wt.% acetylene black and 10 wt.% carboxymethylcellulose. Copper foil was used as the current collector. Galvanostatic charge/discharge measurements were performed using a multichannel battery testing system (LAND CT2001A). Cyclic voltammograms (CV, 0.01-3 V) and electrochemical impedance spectra (EIS) were collected using an Autolab potentiostat/galvanostat. Specific capacities were calculated based on the mass of active material. The mass loading of each electrode was 1-1.5 mg cm^{-2} .

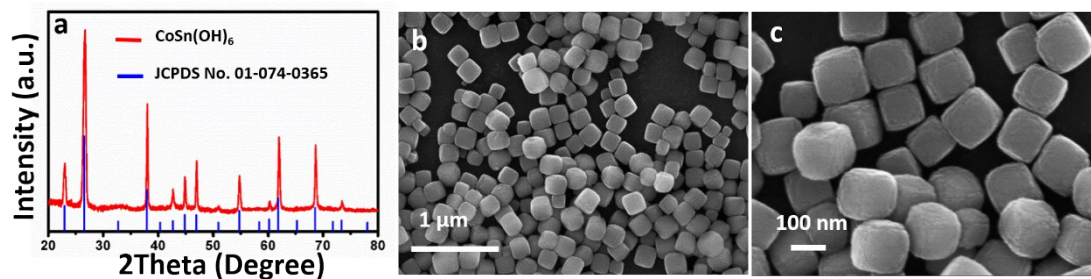


Fig. S1 (a) XRD pattern, (b, c) SEM images of the initial product CoSn(OH)_6 .

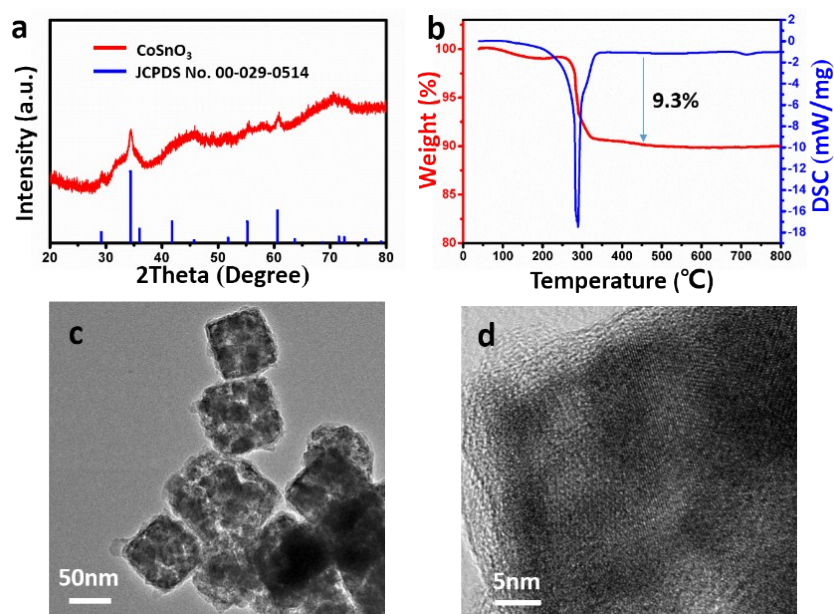


Fig. S2 (a) XRD pattern (b) TG curves and (c, d) TEM images of $\text{CoSnO}_3@\text{NC}$.

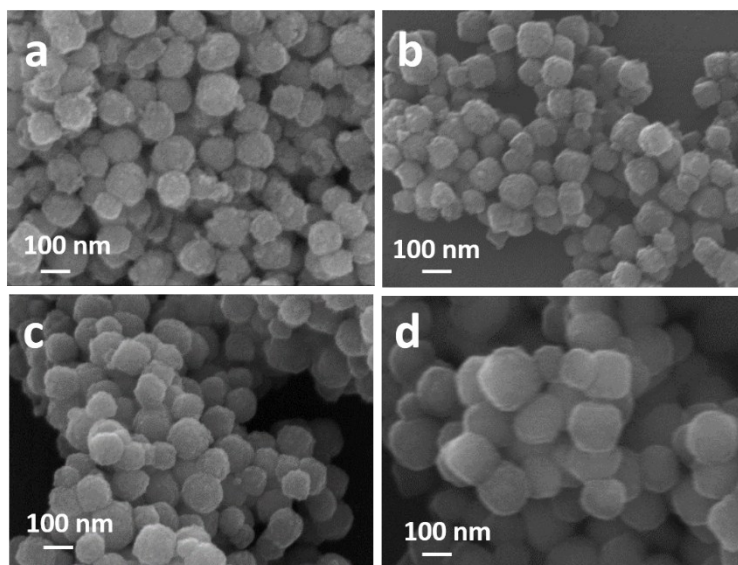


Fig.S3 SEM images of SnO₂@NC-1 (a), SnO₂@NC-1.2 (b), SnO₂@NC-1.5 (c), SnO₂@NC-2 (d).

Tab. S1 ICP results of SnO₂@NC-1.

| | Gauged molar concentration (mmol g ⁻¹) | Ratio (Sn/Co) |
|----|---|------------------|
| Co | 0.143 | 10.3 |
| Sn | 1.478 | |

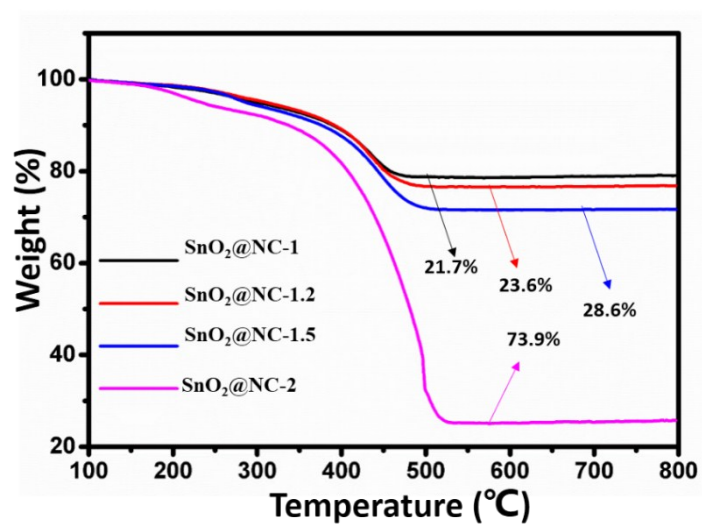


Fig. S4 TG curves of SnO₂@NC.

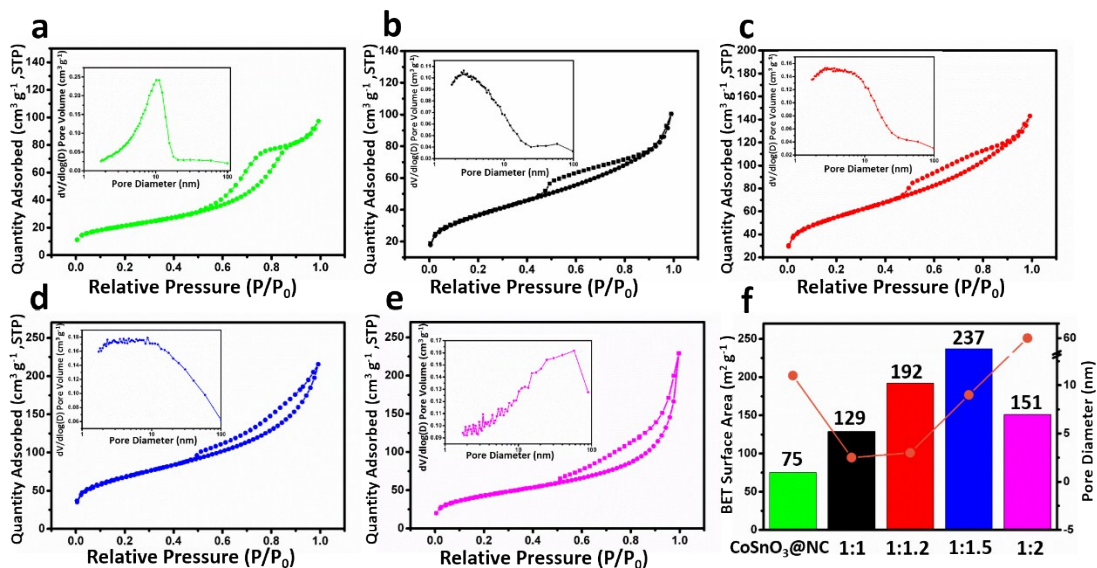


Fig.S5 N_2 adsorption-desorption isotherms of $\text{CoSnO}_3\text{@NC}$ (a), $\text{SnO}_2\text{@NC-1}$ (b), $\text{SnO}_2\text{@NC-1.2}$ (c), $\text{SnO}_2\text{@NC-1.5}$ (d) and $\text{SnO}_2\text{@NC-2}$ (e), respectively. The inserted pictures are the corresponding BJH pore size distribution plots; (f) BET specific surface area of $\text{CoSnO}_3\text{@NC}$ and $\text{SnO}_2\text{@NC}$ and corresponding most probable distribution of pore diameter.

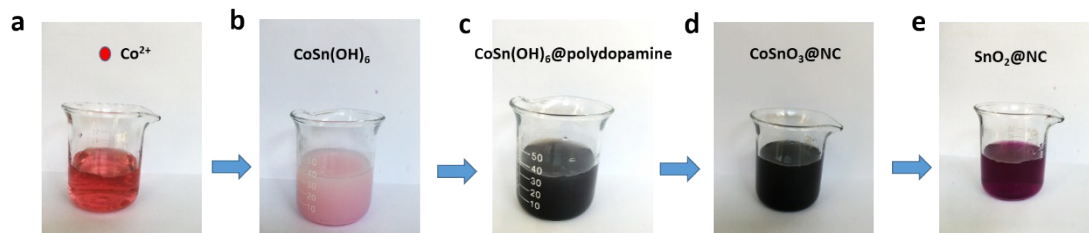


Fig. S6 Digital photo of colour change during the process: (a) aqueous solution after adding all the agents except NaOH; (b) aqueous turbid liquid of as-prepared $\text{CoSn}(\text{OH})_6$; (c) aqueous turbid liquid of $\text{CoSn}(\text{OH})_6\text{@polydopamine}$; (d) aqueous turbid liquid of $\text{CoSnO}_3\text{@NC}$; (e) supernatant after EDTA chelating $\text{CoSnO}_3\text{@NC}$.

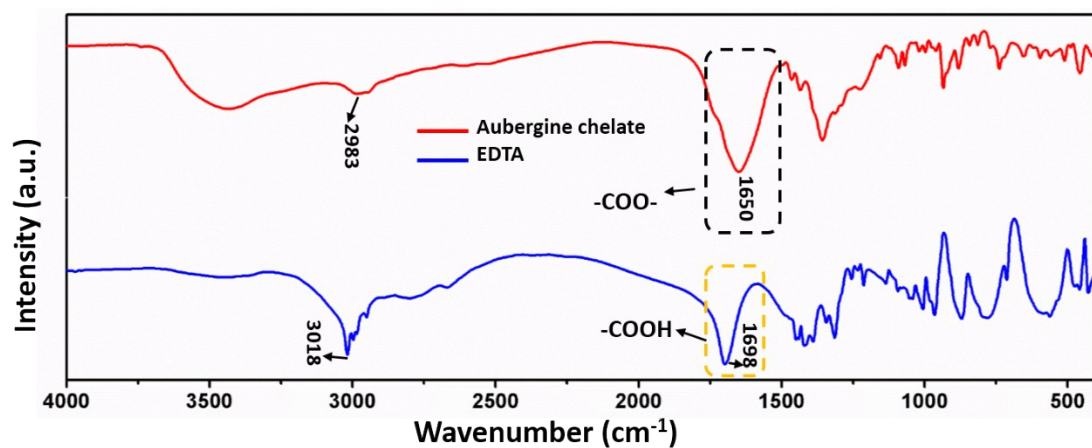


Fig. S7 Fourier transform infrared spectroscopy of EDTA and the aubergine chelate of SnO₂@NC-1.2 after chelation.

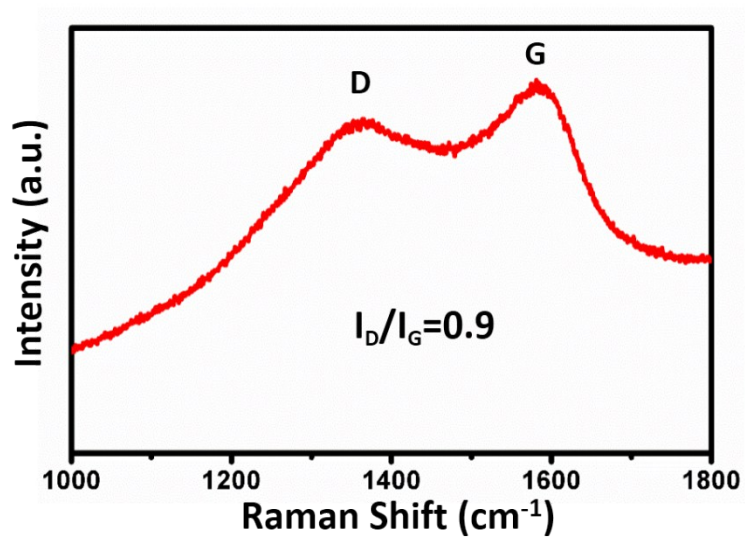


Fig. S8 Raman spectrum of SnO₂@NC-1.2.

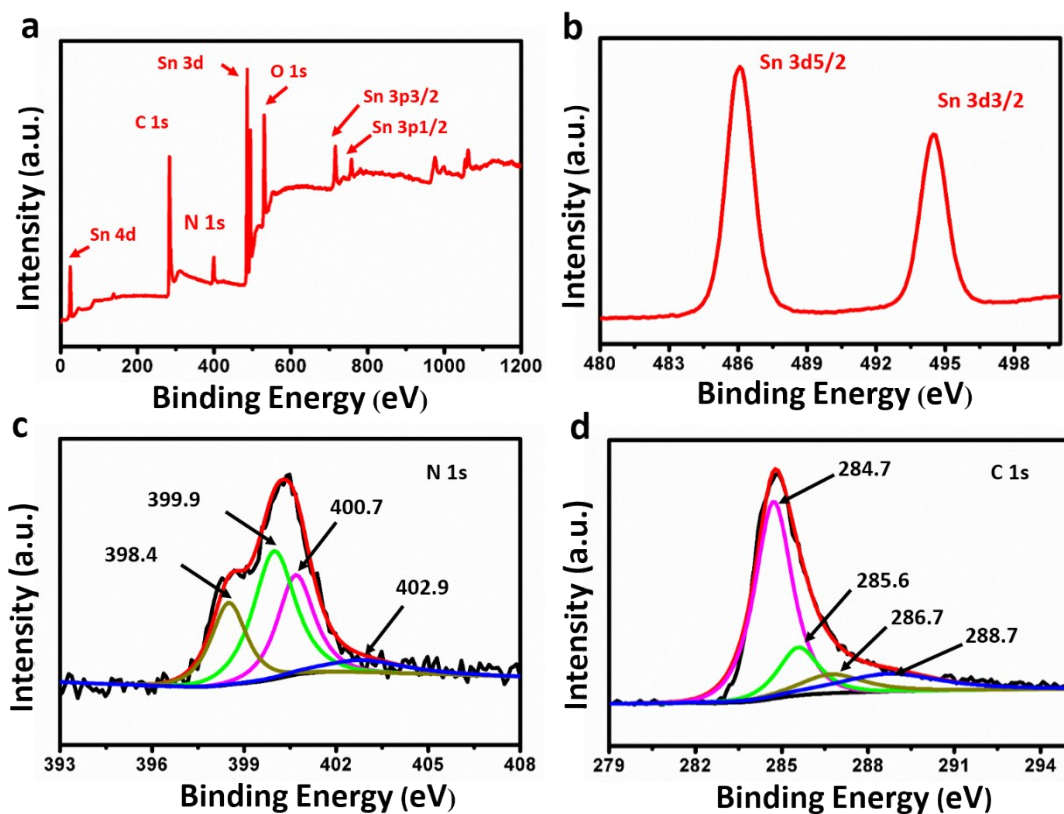


Fig. S9 XPS analysis of SnO₂@NC-1.2 : (a) the survey spectrum, (b) XPS Sn 3d spectra, (c) high-resolution spectrum of N 1s, (d) C 1s spectrum.

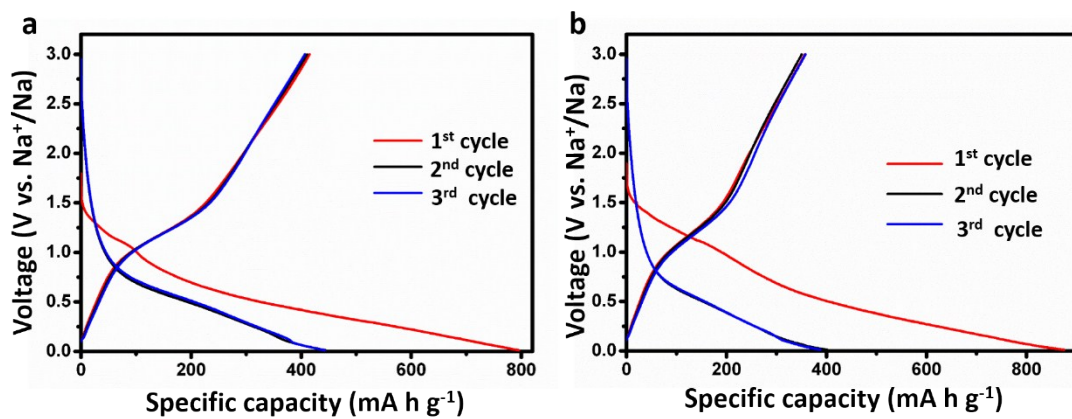


Fig. S10 Charge–discharge profiles of (a) SnO₂@NC-1 and (b) SnO₂@NC-1.5 at a current density of 50 mA g⁻¹ respectively.

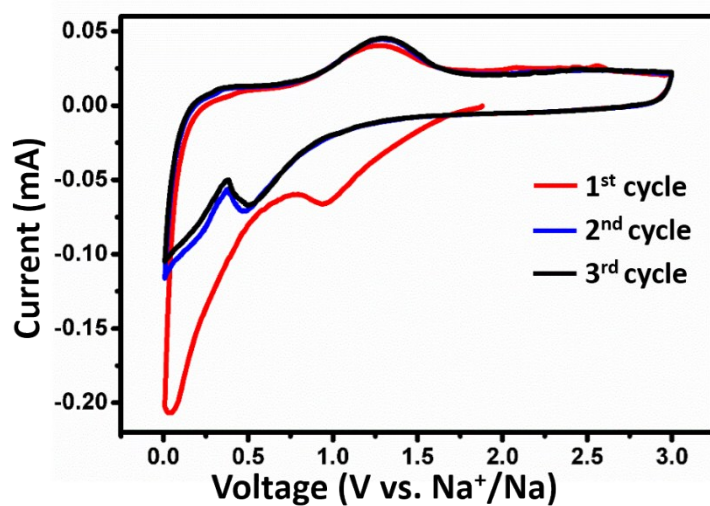


Fig. S11 Cyclic voltammograms at 0.1 mV s^{-1} sweep rate of $\text{SnO}_2@\text{NC-1.2}$ electrode for the first three cycles.

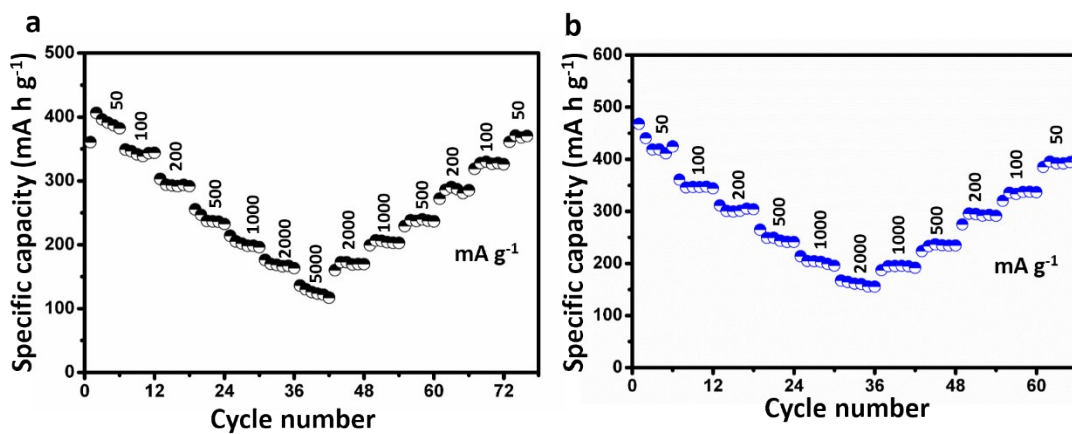


Fig. S12 Rate performance of (a) $\text{SnO}_2@\text{NC-1}$ and (b) $\text{SnO}_2@\text{NC-1.5}$ at various current densities, respectively.

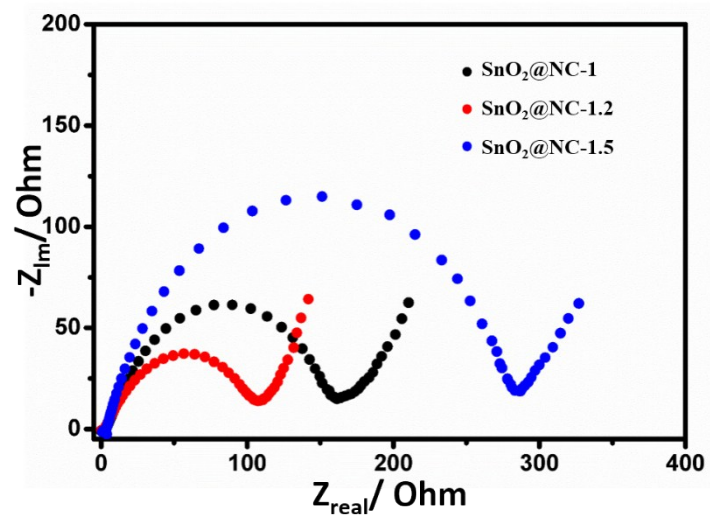


Fig. S13 Nyquist plots of SnO₂@NC electrode after 80 cycles at a current density of 1000 mA g⁻¹.

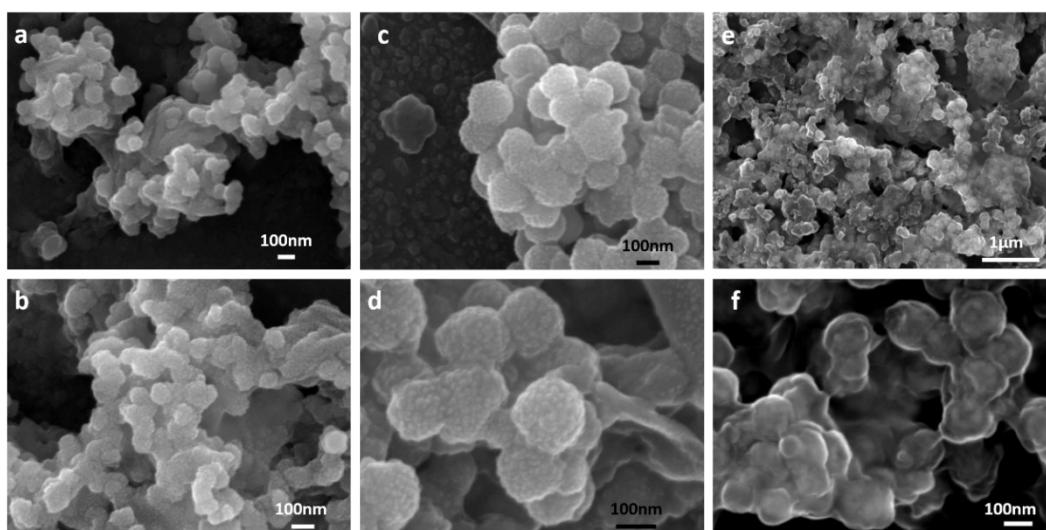


Fig. S14 SEM images of (a, b) SnO₂@NC-1, (c, d) SnO₂@NC-1.2 and (e, f) SnO₂@NC-2 electrode after 80 cycles at a current density of 1000 mA g⁻¹.

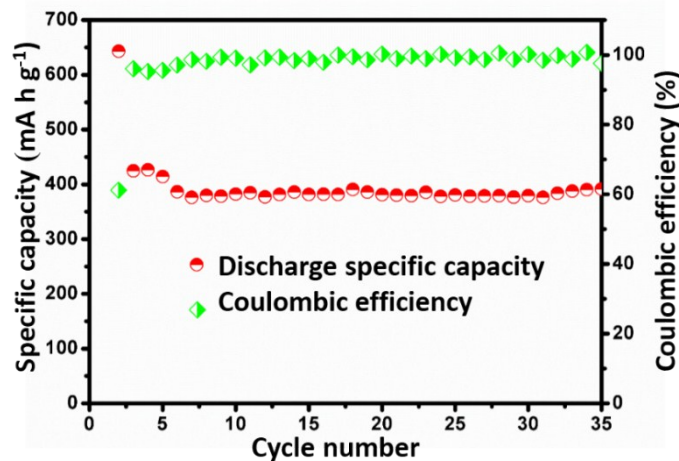


Fig. S15 Cycling performance and coulombic efficiency of SnO₂@NC-1.2 at a current density of 200 mA g⁻¹.

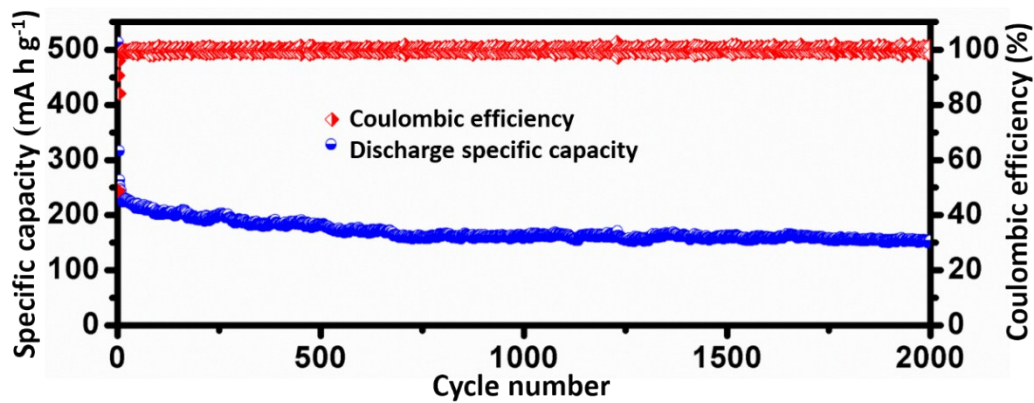


Fig. S16 Cycling performance and coulombic efficiency of SnO₂@NC-1.2 at a current density of 2000 mA g⁻¹. (The electrode was activated at a current density of 50 mA g⁻¹ for the first three cycles.)

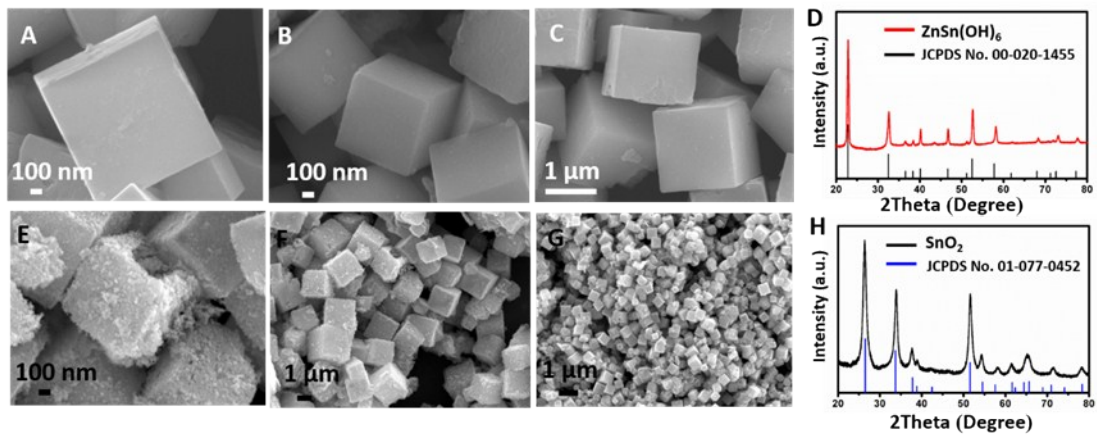


Fig. S17 (A, B, C) SEM images and (D) XRD pattern of ZnSn(OH)_6 , (E, F, G) SEM images and (H) XRD pattern of the obtained SnO_2 .

Table S2. Summary of the representative SnO₂-based anode materials for SIBs.

| Materials | SnO ₂ content wt.% | R _{low} ^{a)} mA h g ⁻¹ /A g ⁻¹ | R _{high} ^{b)} mA h g ⁻¹ /A g ⁻¹ | C ^{c)} mA h g ⁻¹ /A g ⁻¹ /cycle | Ref |
|--|----------------------------------|---|--|---|------------------|
| SnO ₂ /nitrogen-doped graphene | 47 | 339/0.02 | 170/0.64 | 246/0.08/100 | 1 |
| Amorphous SnO ₂ /graphene aerogel | 50.7 | 576.2/0.05 | 84.4/0.8 | 380.2/0.05/100 | 2 |
| SnO ₂ /CNT | 72 | 630.4/0.1 | 324.1/1.6 | 223.2/1.6/300 | 3 |
| SnO ₂ /graphene | 80 | 512/0.05 | 34/0.5 | 220/0.1/100 | 4 |
| SnO ₂ -Graphene DualAerogel | 70 | 448/0.05 | 184/1 | 221/0.2/200 | 5 |
| SnO ₂ @3D graphene | 71.5 | 551/0.05 | 210/0.8 | 432/0.1/200 | 6 |
| Mesoporous NiO/SnO ₂ @rGO | 74.6 | No data | No data | 254.8/0.05/40 | 7 |
| Triple-walled SnO ₂ @N-doped carbon@SnO ₂ nanotubes | 70.4 | 586/0.025 | 320/0.4 | 492/0.025/50 | 8 |
| SnO ₂ -carbon | 60 | 459/0.08 | 133/5.12 | 371/0.08/200 | 9 |
| Ultrafine SnO ₂ -RGO | 76.4 | 480/0.05 | 125/1 | 330/0.1/150 | 10 |
| Carbon/SnO ₂ /carbon cloth | No data | 501/0.134 | 394/6.7 | 314/0.134/100 | 11 |
| Al ₂ O ₃ /SnO ₂ /carbon cloth | No data | 455/0.134 | 245/6.7 | 377/0.134/100 | 11 |
| Mesoporous Sn/SnO ₂ | No data | 500/0.05 | 209.8/1 | 372.3/0.05/50 | 12 |
| Hollow SnO ₂ /SnS ₂ | No data | 497.8/0.3 | 245.4/2.5 | 485.6/0.3/100 | 13 |
| Sn ₂ Nb ₂ O ₇ /SnO ₂ @3D carbon nanocomposites | 60.38 | 302/0.1 | 135/5 | 210/1/500 300/0.1/100 | 14 |
| SnO ₂ /3D graphene | 75 | 321/0.08 | 266/1.2 | 223/0.08/350 | 15 |
| Mesoporous ultrafine SnO₂@N-doped carbon | 76.4 | 560/0.05 | 236/2 180/5 | 255.4/1/1000 385/0.2/35 | This work |

a) Rate performance at low current density; b) rate performance at high current density; c) cycling performance.

References

1. X. Xie, D. Su, J. Zhang, S. Chen, A. K. Mondal and G. Wang, *Nanoscale*, 2015, **7**, 3164-3172.
2. L. Fan, X. Li, B. Yan, J. Feng, D. Xiong, D. Li, L. Gu, Y. Wen, S. Lawes and X. Sun, *Adv. Energy Mater.*, 2016, **6**, 1502057.
3. J. Cui, Z. Xu, S. Yao, J. Huang, J. Huang, S. Abouali, M. A. Garakani, X. Ning and J. Kim, *J. Mater. Chem. A*, 2016, **4**, 10964-10973.
4. H. Lai, B. Feng, Y. Jiang, N. Shi, C. Liang, S. Chang, S. Guo, B. Cui and H. Cao, *Mater. Lett.*, 2016, **166**, 292-295.
5. Z. Li, J. Ding, H. Wang, K. Cui, T. Stephenson, D. Karpuzov and D. Mitlin, *Nano Energy*, 2015, **15**, 369-378.
6. L. Pei, Q. Jin, Z. Zhu, Q. Zhao, J. Liang and J. Chen, *Nano Res.*, 2014, **8**, 184-192.
7. Y. He, A. Li, C. Dong, C. Li and L. Xu, *Chem. Eur. J.*, 2017, **23**, 13724-13733.
8. J. Yue, W. Wang, N. Wang, X. Yang, J. Feng, J. Yang and Y. Qian, *J. Mater. Chem. A*, 2015, **3**, 23194-23200.
9. J. Ding, Z. Li, H. Wang, K. Cui, A. Kohandehghan, X. Tan, D. Karpuzov and D. Mitlin, *J. Mater. Chem. A*, 2015, **3**, 7100-7111.
10. Y. Wang, Y. Lim, M. Park, S. Chou, J. Kim, H. Liu, S. Dou and Y. Kim, *J. Mater. Chem. A*, 2014, **2**, 529-534.
11. Y. Liu, X. Fang, M. Ge, J. Rong, C. Shen, A. Zhang, H. A. Enaya and C. Zhou, *Nano Energy*, 2015, **16**, 399-407.
12. D. Tang, Q. Huang, R. Yi, F. Dai, M. L. Gordin, S. Hu, S. Chen, Z. Yu, H. Sohn, J. Song and D. Wang, *Eur. J. Inorg. Chem.*, 2016, **13-14**, 1950-1954.
13. K. Wang, Y. Huang, X. Qin, M. Wang, X. Sun and M. Yu, *ChemElectroChem*, 2017, **4**, 1-7.
14. P. Zhai, J. Qin, L. Guo, N. Zhao, C. Shi, E. Liu, F. He, L. Ma, J. Li and C. He, *J. Mater. Chem. A*, 2017, **5**, 13052-13061.
15. J. Lee, J. Song, Y. Cha, S. Fu, C. Zhu, X. Li, Y. Lin and M. Song, *Nano Res.*, 2017, 1-17.